

## Polarimetric Scanning Radiometer for Airborne Microwave Imaging Studies

Jeffrey R. Piepmeier and A. J. Gasiewski

School of Electrical and Computer Engineering  
Georgia Institute of Technology, Atlanta, GA 30332-0250  
(404) 894-2984; (404) 894-2934; FAX (404) 894-4641  
gt2930b@prism.gatech.edu ; ag14@prism.gatech.edu

**Abstract** - A multiband microwave polarimetric scanning radiometer (PSR) has been constructed for airborne observations from the NASA DC-8 airborne platform. The primary application of the PSR is the development of optimal spaceborne hardware configurations and retrieval algorithms for passive wind-vector sensing over the ocean surface. Four radiometers, operating at 10.7, 18.7, 37, and 89 GHz, each measure the first three modified Stokes' parameters ( $T_v$ ,  $T_h$ , and  $T_U$ ). A gimballed mechanism allows observations at any incident angle within a cone of  $\sim 70^\circ$  half-angle around nadir. The PSR's four radiometers and two-axis scanning capability will provide unique polarimetric data for microwave emission studies of both ocean and land surfaces, as well as atmospheric clouds and precipitation.

### 1. INTRODUCTION

Airborne remote sensing instruments can provide critical data needed for spaceborne sensor and retrieval algorithm development. Given the recent mandates for low-cost Earth probes, airborne measurements have become all the more important to such development. Indeed, for only a small fraction of the cost of a comparable spaceborne system, an airborne sensor can provide a wealth of data for determining the optimal configuration of spaceborne hardware and geophysical estimation algorithms. We describe here a new instrument for passive microwave remote sensing from airborne platforms which provides several unique capabilities. The Polarimetric Scanning Radiometer (PSR) was developed to provide wideband spectral coverage with tri-polarimetric (three Stokes' parameter) capability using a variety of scan modes. The primary application of the PSR is the development of optimal hardware configurations and retrieval algorithms for passive wind-vector sensing over the ocean surface. Additional applications include high-resolution polarimetric imaging of clouds, convective precipitation, sea ice, and (to a lesser degree) soil moisture.

### 2. INSTRUMENT DESCRIPTION

This work was supported by ONR grant N00014-95-1-0426, NASA grant NAGW 4191, and the Georgia Institute of Technology.

The PSR consists of four gimbal-mounted radiometers operating at 10.7, 18.7, 37, and 89 GHz (Figure 1). Each radiometer measures the first three modified Stokes' parameters ( $T_v = \langle |E_v|^2 \rangle$ ,  $T_h = \langle |E_h|^2 \rangle$ , and  $T_U = 2\text{Re}(E_v E_h^*)$ ). Analog detection hardware is used to measure the orthogonal brightness temperatures,  $T_v$  and  $T_h$ . A recently developed three-level digital correlator operating at 1 GS/s has been implemented for the measurement of  $T_U$ . This combination of receiver/detector technology allows precise calibration using only two (hot and cold) non-polarized calibration standards.

A dual-band feedhorn antenna with integrated lens provides 3-dB beamwidths of  $8^\circ$  and  $2.3^\circ$  at 10.7 and 37 GHz, respectively. The antenna uses a corrugated scalar feedhorn along with a grooved rexolite lens. Orthomode couplers are used to obtain the orthogonally-polarized signals. Two similar single-band lens/feedhorn antennas operating at 18.7 and 89 GHz have 3-dB beamwidths of  $8^\circ$  and  $2.3^\circ$ , respectively. These beamwidths correspond to nadir spot sizes from 200 to 700 meters when operated at a nominal altitude of 5 km. Polarization isolation within the principal planes is typically better than 30 dB. While conventional double sideband superheterodyne radiometers are used for the 37 and 89 GHz channels, single sideband receivers with HEMT front-end amplifiers are used for the 10.7 and 18.7 GHz channels. Other important radiometric specifications are provided in Table 1. The block diagram for the typical PSR radiometer is shown in Figure 2.

The digital correlators are comprised of three basic components: (1) high-speed analog-to-digital converters (ADC), (2) three-level multipliers, and (3) ripple accumulators. The baseband radiometer signals are sampled and quantitized into three levels at  $10^9$  samples per second. Following discretization, the signal samples are multiplied and the resulting products are accumulated in a 24-bit ripple counter. The accumulated value is converted into an estimated analog correlation coefficient using methods presented in [1]. With the appropriate threshold levels, the three level correlator achieves a sensitivity of  $\sim 0.81$  relative to a perfect analog correlator [2].

The correlators use discrete high-speed ECL components to achieve a fast sampling rate and wide bandwidth. The high-speed ECL signals exhibit transition times of

DTIC QUALITY INSPECTED 4

DISTRIBUTION STATEMENT A  
Approved for Public Release  
Distribution Unlimited

19990723 022

$\lesssim 250$  ps; therefore, the digital signals have spectral content  $\geq 4$  GHz. The circuit is fabricated on low-loss woven PTFE double-sided copper-clad circuit board. All high-speed components (both passive and active) are surface mount devices. Microstrip transmission lines with terminating resistors form signal interconnections. The use of such microwave digital design techniques eliminates ringing and minimizes transition time, thus maximizing the correlator bandwidth. When sampled at the Nyquist rate, each correlator measures an IF band of width 500 MHz. The use of several correlators along with IF sub-band splitting hardware provides a total IF channel bandwidth equal to a multiple of the bandwidth for a single correlator.

The PSR gimbal structure allows the radiometer antennas to be scanned in-flight using two independent degrees of freedom (azimuth and elevation). The mechanism permits a number of scanning modes, including conical, cross-track, and spot-light modes. These scan modes may include any observation angle within a cone of  $\sim 70^\circ$  half-angle around nadir. (A fence is located in front of the instrument to reduce wind loading; this fence limits the direct forward view to  $\sim 53^\circ$  from nadir.) A programmable controller operates two sealed, low-temperature stepper motors with position feedback obtained using two 12-bit optical encoders providing  $0.088^\circ$  pointing knowledge.

Electrical power is supplied to the instruments in the drum via slip-rings, thus allowing continuous rotation of the radiometer drum in both axes. Maximum motor torque is  $\sim 75$  N·m (100 ft·lbf), providing a minimum scan rate of one line every three seconds. Passive motor brakes are used to prevent windmilling in the event of power loss.

Calibration of the PSR is accomplished by viewing two unpolarized blackbody standards, one at ambient temperature ( $\sim 250$  K) and one heated to  $\sim 310$  K. Each standard consists of absorber material fastened to a metal heat sink and contained within a closed-cell styrofoam insulating jacket. Using the digital correlator, only two such calibration standards (hot and cold) are needed to calibrate both the total power channels ( $T_v$  and  $T_h$ ) and the cross-correlating channel ( $T_U$ ). Blackbody temperatures are measured at eight locations on each standard using RTD sensors embedded in the absorbing material. The scanhead drum, slip rings, and calibration loads are purged in-flight with dry nitrogen to protect the radiometers, electronics, and other sensitive materials from water vapor and condensation.

Radiometric data is collected by a computer located within the scanning drum. This remote system communicates with the main computer via a 10-base-2 local area network. The main computer system, used for interac-

tive experiment control and data logging, is located in the cabin of the aircraft. Temperature data from the calibration standards is stored in a RAM cache and transferred via an RS232 interface for storage by the data acquisition system. Data from the various sources are time-stamped using time generators synchronized to IRIG-B signals, thus facilitating precise temporal registration. A video camera is located within the scanhead and co-boresighted with the radiometer antennas.

### 3. APPLICATIONS

Dual-polarized radiometer data from the DMSP SSM/I instrument has been shown to be useful for the measurement of the oceanic wind vector [3]. Recently, the utility of  $T_U$  was experimentally observed by [4, 5]. Specifically, azimuthal brightness variations of  $T_U$  were shown to be similar in amplitude to those of  $T_v$  and  $T_h$ , but in phase quadrature.  $T_U$  appears to be relatively insensitive to unpolarized emissions from clouds. The paucity of available polarimetric data, however, has hindered the development of an optimal passive wind-vector sensor. The PSR is unique in that it is the first aircraft instrument designed to both verify and help improve passive wind vector sensing techniques applicable to spaceborne observation systems. Importantly, images of the upwelling Stokes parameters can be made over a wide microwave frequency range (X- to W-band) with channels comparable to the SSM/I, SSM/I-S, and EOS MIMR sensors, and over a wide range of surface incident angles. Thus, the conically scanned imagery from the PSR will be critical to both the development of wind vector retrieval algorithms and the optimal configuration for a spaceborne wind vector sensor.

Since the launch of the first SSM/I in 1987, this instrument has been used to map convective precipitation rate, cloud liquid water, ice content, and integrated water vapor, along with sea surface parameters. Improvements in global equatorial coverage could be obtained using a slightly wider cone-angle than provided by the SSM/I. The requirement of global equatorial coverage at the SSM/I altitude of 833 km in turn requires a greater surface incident angle ( $\sim 63^\circ$ ). Underflights of the SSM/I using the PSR will be useful in assessing the impact of such an increase in the angle of incidence on the accuracy of the above retrieved parameters. In addition, the PSR will be useful as a post-launch underflight sensor for calibration and validation purposes.

### 4. SUMMARY

PSR components are currently being assembled at the Georgia Institute of Technology, with initial flights being

planned for May-June, 1996. A second set of lights focussing on passive wind vector sensing is being planned for January 1997 over the Labrador Sea area. With its multispectral polarimetric measurement capabilities the PSR will provide important data necessary for the development of passive wind-vector sensing techniques. Future deployments of the PSR are being planned in conjunction with the NASA Tropical Rainfall Measurement Mission (TRMM) and with calibration/validation studies in support of the National Polar-Orbiting Operational Environmental Satellite System (NPOESS).

**Acknowledgements:** The authors would like to thank R. Davidson, J. Baloun, and M. Tucker of the Raytheon Corporation; C. Campbell, E. Panning, D. Kunkee, E. Thayer, and S. Sharpe of the Georgia Institute of Technology for valuable contributions to the design of the PSR; and Dr. M. Van Woert of the U.S. Office of Naval Research for his support.

## REFERENCES

- [1] S. R. Kulkarni and C. Heiles, "How to obtain the true correlation from a 3-level digital correlator", *The Astronomical Journal*, vol. 85, no. 10, pp. 1413-1420, October 1980.
- [2] B. F. C. Cooper, "Correlators with two-bit quantization", *Aust. J. Phys.*, vol. 23, pp. 521-527, 1970.
- [3] F. J. Wentz, "Measurement of oceanic wind vector using satellite microwave radiometers", *IEEE Trans. Geosci. Remote Sensing.*, vol. 30, no. 5, pp. 960-972, September 1992.
- [4] S. Yueh, W. Wilson, F. Li, S. Nghiem, and W. Ricketts, "Polarimetric measurements of sea surface brightness temperatures using an aircraft K-band radiometer", *IEEE Trans. Geosci. Remote Sensing.*, vol. 33, no. 1, pp. 85-92, January 1995.
- [5] A. J. Gasiewski and D. B. Kunkee, "Polarized microwave emission from water waves", *Radio Sci.*, vol. 29, no. 6, pp. 1449-1466, December 1994.

**Table 1. Radiometer specifications**

| Band                                  | X         | Ku        | K           | W           |
|---------------------------------------|-----------|-----------|-------------|-------------|
| Frequency (GHz)                       | 10.4-10.8 | 18.4-19.0 | 36-38       | 86-92       |
| Receiver type                         | SSB/HEMT  | SSB/HEMT  | DSB/LO      | DSB/LO      |
| IF bandwidth (MHz)                    | 400       | 500       | 1000        | 2000        |
| Receiver temp. (K)                    | 250       | 350       | 550         | 800         |
| Sensitivity (K) for 10 ms integration | 0.24      | 0.29      | 0.27        | 0.24        |
| 3-dB beamwidth                        | 8°        | 8°        | 2.3°        | 2.3°        |
| 3-dB spot size (km) at 5 km altitude: |           |           |             |             |
| nadir                                 | 0.70      | 0.70      | 0.20        | 0.20        |
| 53° incidence                         | 1.1 x 1.9 | 1.1 x 1.9 | 0.32 x 0.55 | 0.32 x 0.55 |

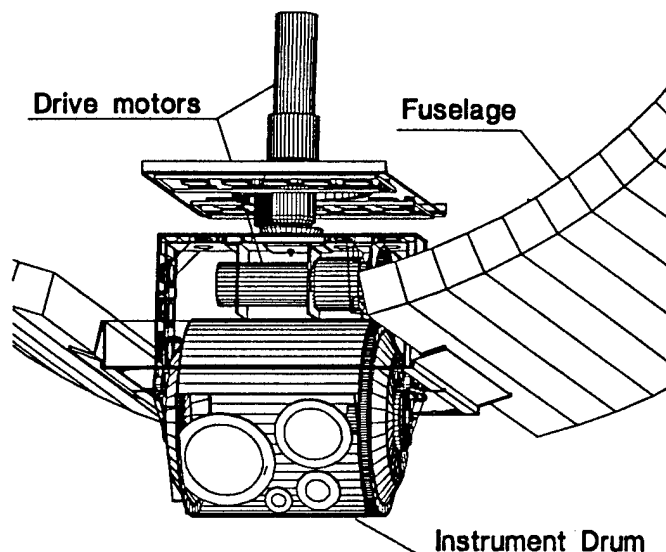


Figure 1: Three-dimensional CAD rendering of PSR illustrating instrument drum and gimbal mount. Support structure has been removed for clarity.

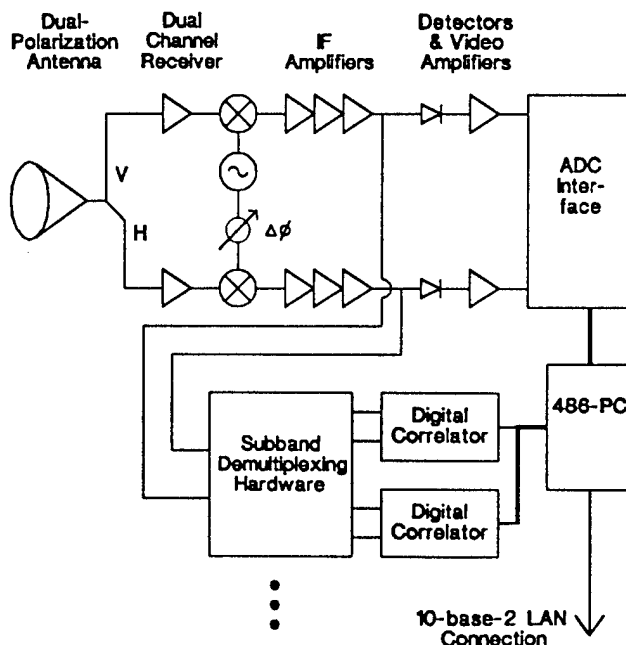


Figure 2: Block diagram of the typical PSR radiometer.